

RESEARCH

Open Access



# Retinoic acid enhances $\gamma\delta$ T cell cytotoxicity in nasopharyngeal carcinoma by reversing immune exhaustion

Guichao Liu<sup>1,2,3†</sup>, Qiang Quan<sup>1,3†</sup>, Lanhong Pan<sup>1,3,4†</sup>, Haibo Duan<sup>1,3†</sup>, Guojun Zhang<sup>1,3</sup>, Ke Li<sup>6</sup>, Xinhai Zhu<sup>1,3\*</sup>, Dongdong Zhang<sup>5\*</sup>, Peng Li<sup>7,8\*</sup> and Jianfu Zhao<sup>1,3\*</sup>

## Abstract

Recent studies have shown that the antitumor immunity of adaptive immune cells is regulated by Vitamin A (retinoic acid, RA). However, it remains unclear whether RA and retinoic acid receptor (RAR) signaling can modulate antitumor immunity by reversing immune exhaustion of innate-like  $\gamma\delta$  T cells in human nasopharyngeal carcinoma (NPC). Periphery blood samples from patients with NPC were prospectively collected, and phenotypic and functional analyses of  $\gamma\delta$  T cells were performed using flow cytometry. Tumor-bearing models and RAR inhibitor approaches were utilized to investigate RA/RAR-mediated regulation of T cell immunoglobulin domain and mucin domain 3 (Tim-3) and the antitumor activity of  $\gamma\delta$  T cells. Here, our findings indicate that immune exhaustion markers are highly expressed on peripheral  $\alpha\beta$  and  $\gamma\delta$  T cells in NPC patients. Serum RA levels are negatively correlated with the abundance of Tim-3 on circulating V $\delta$ 2 T cells. Mechanistic studies have demonstrated that RA/RAR signaling directly targets V $\delta$ 2 T cells, repressing Tim-3 expression, promoting NF- $\kappa$ B activation, and enhancing the production of anti-tumor-related cytokines. Notably, RA supplementation improved the efficacy of V $\delta$ 2 T cell-mediated immunotherapy in human NPC by suppressing Tim-3 expression. Collectively, these findings suggest that RA/RAR signaling plays a crucial role in reversing immune exhaustion and represents a promising target for  $\gamma\delta$  T cell antitumor immunotherapy.

**Keywords**  $\gamma\delta$  T cells, Retinoic acid, Retinoic acid receptor, Tim-3, Tumor immunity

<sup>†</sup>Guichao Liu, Qiang Quan, Lanhong Pan and Haibo Duan contributed equally to this work.

\*Correspondence:

Xinhai Zhu  
robin82613@163.com  
Dongdong Zhang  
zhangdd@jnu.edu.cn  
Peng Li  
pengli1991@jnu.edu.cn  
Jianfu Zhao  
zhaojianfu@jnu.edu.cn

<sup>1</sup> The First Affiliated Hospital, Jinan University, Guangzhou, China

<sup>2</sup> Department of Radiation Oncology, The First People's Hospital of Foshan City, Foshan, China

<sup>3</sup> Department of Oncology, Research Center of Cancer Diagnosis and Therapy, The First Affiliated Hospital, Jinan University, Guangzhou, China

<sup>4</sup> Department of Ultrasound Medicine, The First Affiliated Hospital, Jinan University, Guangzhou, China

<sup>5</sup> Department of Thoracic Surgery, The First Affiliated Hospital, Jinan University, Guangzhou, China

<sup>6</sup> Department of Geriatrics, The Seventh Affiliated Hospital, Sun Yat-Sen University, Shenzhen, China

<sup>7</sup> Guangdong Provincial Key Laboratory of Tumor Interventional Diagnosis and Treatment, Zhuhai Institute of Translational Medicine, Zhuhai People's Hospital Affiliated with Jinan University, Jinan University, Zhuhai, China

<sup>8</sup> Faculty of Medical Science, The Biomedical Translational Research Institute, Jinan University, Guangzhou, China



## Introduction

Nasopharyngeal carcinoma (NPC), a small proportion of head and neck cancers, is one of the most prevalent tumors in Southeast Asia and southern China especially in Guangdong province [1–5]. In general, dietary habits, genetic factors, and Epstein-Barr virus (EBV) infection are associated with NPC etiology [6–9]. Most patients with NPC are sensitive to radiotherapy [10]. However, distant metastasis and tumor recurrence occur in some NPC patients despite treatment with radiotherapy and chemotherapy [8, 11]. One of the critical reasons is that the patient's immune cells are exhausted, resulting in impaired antitumor immunity of T cells in the tumor microenvironment (TME) [9, 12].

Tumor tissue is infiltrated by multiple types of immune cells that contain adaptive (CD4, CD8) T cells and innate immune cells (natural killer cells, NK), and provide one of the major protections in antitumor immunity [13, 14]. Moreover, innate-like  $\gamma\delta$  T cells, especially the human V $\gamma$ 9V $\delta$ 2 (V $\delta$ 2) T cell subpopulation, which is independent of the major histocompatibility complex (MHC), can directly recognize and lyse tumor cells by producing cytokines, such as IFN- $\gamma$ , TNF- $\alpha$ , Perforin and Granzyme B, to initiate cytotoxicity against tumor cells [15–19]. The abundance of tumor-infiltrating  $\gamma\delta$  T cells is the best prognostic marker of patient survival [20]. Several trials have demonstrated that V $\gamma$ 9V $\delta$ 2 T cell immunotherapy exhibits promising clinical safety and prolongs the survival of patients with late-stage cancer [21, 22]. However, persistent exposure to cancer antigens without appropriate activation triggers T cell exhaustion and limits their application in tumor immunotherapy [23–25].

The TME suppresses T cell effector functions by inducing immune inhibitory receptors such as programmed cell death 1 (PD-1), Tim-3, and T-cell immunoreceptor with Ig and ITIM domains (TIGIT) on T cells [26–28]. These hallmarks of T cell exhaustion are often associated with immune dysfunction and unresponsiveness in tumor [14, 29]. Unfortunately, only few patients can benefit from immune checkpoint blockade therapies, the pivotal reason is that their immune cells are abnormal and severely exhausted in long-term tumor pressure [14, 30]. Recently, Evan W. Weber et al. showed that transient rest restores functionality in exhausted chimeric antigen receptor T cells (CAR-T) through epigenetic remodeling, indicating that alleviating T cell exhaustion using small molecules is a promising approach for the sustained control of tumor progression [31].

The vitamin family is crucial for the physiological functions of the human body [32]. Several studies have suggested that retinoic acid (RA), a major active formula metabolite of vitamin A, plays a key role in the

differentiation or antitumor immunity of T cell subsets and other immune cells [33–40]. Although CD4 and CD8 T cell function has been well-established and considered a target of immunotherapy for cancer patients, relatively few studies have focused on the importance of small molecules, especially vitamin A treatment, in alleviating immune exhaustion and promoting the antitumor immunity of  $\gamma\delta$  T cells.

In this study, low serum RA levels were associated with high levels of Tim-3 in circulating V $\delta$ 2 T cells in patients with NPC. We demonstrated that treatment with RA reduced Tim-3 expression while promoting the production of IFN- $\gamma$  and TNF- $\alpha$  in V $\delta$ 2 T cells, resulting in enhanced immunotherapy efficacy. These findings indicate that RA has the potential to optimize  $\gamma\delta$  T-cell antitumor immunotherapy in NPC patients.

## Methods

### PBMCs isolation

Peripheral blood mononuclear cells (PBMCs) were isolated by density gradient centrifugation (Cytiva, 17,144,002) [41] from diagnosed NPC patients and age-matched healthy donors (HD), who were recruited from the First People's Hospital of Foshan, China. All experimental procedures, involving PBMCs samples from NPC patients and healthy donors were approved by the Institutional Review Board of the First People's Hospital of Foshan, Foshan, P. R. China (approval number, FSYYY-EC-SOP-008–02.0-A09). Detailed information on the healthy donors and NPC patients is provided in Supplementary Table 1.

### In vitro assays

To assess immune exhaustion and costimulatory markers, zoledronic acid (ZOL)-expanded V $\delta$ 2 T cells were treated with 250 nM all-trans-retinoic acid (RA; MCE, HY-14649) or Vehicle three times at 1-day intervals, followed by flow cytometry analysis. To detect intracellular antitumor-related cytokines, ZOL-expanded V $\delta$ 2 T cells were treated with Vehicle, 250 nM RA, and 100 nM AGN 193109 (retinoic acid receptor inhibitor, RARi; MCE, HY-U00449) either alone or in combination for 24 h. The cells were then treated with 50 ng/mL phorbol 12-myristate 13-acetate (PMA; Sigma, P8139) and 1  $\mu$ g/mL ionomycin (Ion; Sigma, I9657) in the presence of Golgi Stop (1:1000 dilution; BD Biosciences, 554,724) for an additional 4 h, followed by flow cytometry detection. In some experiments, V $\delta$ 2 T cells were treated with Vehicle, 250 nM RA, and 100 nM AGN 193109 either alone or in combination for 24 h, and surface markers were analyzed by flow cytometry.

### Flow cytometry

To further investigate the surface and intracellular markers in T cells, the following monoclonal antibodies (mAbs) were used: V500 anti-human CD3 (BD Biosciences, 561,416; UCHT1), PerCP anti-human CD4 (BioLegend, 317,431; OKT4), FITC anti-human CD8 (BioLegend, 344,703; SK1), PerCP anti-human V $\delta$ 2 (BioLegend, 331,410; B6), FITC anti-human V $\delta$ 1 (Miltenyi; REAL277), Brilliant Violet 421<sup>TM</sup> anti-human PD-1 (BioLegend, 329,920; EH12.2H7), APC anti-human Tim-3 (BioLegend, 345,011; F38-2E2), PE anti-human Tim-3 (BioLegend, 345,005; F38-2E2), PE/Cyanine7 anti-human TIGIT (BioLegend, 372,714; A15153G), PE anti-human CD28 (BioLegend, 302,907; CD28.2), APC anti-human IFN- $\gamma$  (BioLegend, 502,512; 4S.B3), PE anti-human TNF- $\alpha$  (BioLegend, 502,909; MAb11), Brilliant Violet 421<sup>TM</sup> anti-human Perforin (BioLegend, 308,121; dG9), PE/Cyanine7 anti-human/mouse Granzyme B (BioLegend, 396,409; QA18A28), PE/Cyanine7 anti-mouse CD3 (BioLegend, 100,220; 17A2), Brilliant Violet 421<sup>TM</sup> anti-mouse TCR $\gamma$  $\delta$  (BioLegend, 118,119; GL3), APC anti-mouse PD-1 (BioLegend, 109,111; RMP1-30), Brilliant Violet 711<sup>TM</sup> anti-mouse CD366 (BioLegend, 119,727; RMT3-23), APC anti-mouse IFN- $\gamma$  (BioLegend, 505,809; XMG1.2), FITC anti-mouse TNF- $\alpha$  (BioLegend, 506,304; MP6-XT22), and Pacific Blue anti-mouse Granzyme B (BioLegend, 515,407; GB11). LIVE/DEAD FIX AQUA—80 (ThermoFisher, L34965) was employed to differentiate between live and dead cells. T Cell phenotypes were determined using flow cytometry (Cytek Aurora) and analyzed via FlowJo v10.

### Immunoblotting

ZOL-expanded V $\delta$ 2 T cells were treated with Vehicle, 250 nM RA, 100 nM AGN 193109, or a combination of RA and RARi for 24 h, followed by stimulation with PMA (50 ng/mL) and Ion (1  $\mu$ g/mL) for an additional another 4 h. The V $\delta$ 2 T cells were lysed in RIPA buffer containing Phosphatase Inhibitor Cocktail (Selleck, B15001) and 1 mM Protease Inhibitor (MCE, HY-B0496) on ice for 35 min. Protein supernatants were collected for further analysis. Total protein (20–40  $\mu$ g) was transferred to 0.45  $\mu$ m polyvinylidene fluoride (PVDF) membranes via western electrotransfer (Bio-Rad). The following primary antibodies were used: p38 MAPK (CST, 8690 T; D13E1), p-p38 MAPK (CST, 4511 T; D3F9), Akt (CST, 4691 T; C67E7), p-Akt (CST, 4060 T; D9E), NF- $\kappa$ B (CST, 8242 T; D14E12), p-NF- $\kappa$ B (CST, 3033 T; 93H1), PLC- $\gamma$ 1 (CST, 2822S; NA), p-PLC- $\gamma$ 1 (14008S; D6M9S), Erk1/2 (CST, 9102S; NA), p-Erk1/2 (CST, 9101S; NA), RAR $\alpha$  (MCE, HY-P80308; NA), RAR $\beta$  (Gene Tex, GTX100759-S; NA), RAR $\gamma$  (Gene Tex, GTX102914-S; NA), and  $\beta$ -actin (CST,

3700; 8H10D10). HRP-conjugated secondary antibodies included anti-mouse IgG, HRP-linked antibody (CST, 7076), anti-rabbit IgG, HRP-linked antibody (CST, 7074). The PVDF membranes were analyzed using the Chemi-Doc MP Gel Imaging System (Bio-Rad) and Image Lab 5.1 software.

### RAR $\alpha$ knockout V $\delta$ 2 T cell and tumor lysis experiment

For RAR $\alpha$  knockout, HEK293T cells were transfected with the packaging plasmids PMD.2G (Addgene, 12,259) and psPAX2 (Addgene, 12,260) along with lenti-CRISPR v.2-based (Addgene, 52,961) knockout vectors, using Lipofectamine 3000 (Thermo Fisher Scientific), according to the manufacturer's instructions. sgRNA sequences were provided in supplemental Table 2. Virus-containing suspension was concentrated overnight using a concentration kit (Clontech, 631,231). V $\delta$ 2 T cells were transduced with lentivirus carrying CRISPR-Cas9-RAR $\alpha$  (KO) and negative control CRISPR-Cas9 (NC), respectively, by centrifugation at 500 g for 90 min at 4°C [12]. T cells were then cultured in normal medium for an additional 2 days. After two rounds of puromycin selection, the cells were harvested and assessed by immunoblotting. Transduced V $\delta$ 2 T cells were subsequently treated with 250 nM RA twice, at 1-day intervals, for a tumor lysis experiment. In some experiments, V $\delta$ 2 T cells (effector, E) and target cells (C666-1/MCF-7/Jurkat, T) were cocultured at the indicated ratios at 37 °C for 6 or 12 h, with or without 15  $\mu$ g/mL  $\alpha$ Tim-3 treatment, and cell lysis was determined using the CytoTox 96 Non-radioactive kit (Promega, G1780).

### Tumor models

For the B16-F0 tumor-bearing model,  $5.0 \times 10^5$  B16-F0 cells were subcutaneously injected into the left flank of 5–6 week-old wild-type (WT) mice. When the tumor volume reached to approximately 50–100 mm<sup>3</sup>, tumor-bearing mice were intraperitoneally injected with 25  $\mu$ g/mouse AGN194310 (RARi; MCE, HY-16681), 2.5 mg/kg retinoic acid (RA; MCE, HY-14649), 150  $\mu$ g/mouse  $\alpha$ TCR $\gamma$  $\delta$  (BioLegend, 107,517), 150  $\mu$ g/mouse anti-CD8a (Selleck, A2102) alone, or RA combined with RARi/ $\alpha$ TCR $\gamma$  $\delta$ / $\alpha$ CD8a four times at three-day intervals. IgG was used as the isotype control for anti-TCR $\gamma$  $\delta$  and anti-CD8a treatments. For the C666-1 tumor model, NOD.Cg-Prkdc<sup>scid</sup>Il2r<sup>gem1</sup>Snoc (M-NSG, Shanghai Model Organisms Center) mice were subcutaneously inoculated with  $1.5 \times 10^6$  C666-1 cells (Guangzhou Laijing Biotechnology Co., Ltd). When the tumor volume reached 50–100 mm<sup>3</sup>, the mice were treated with 2.5 mg/kg RA,  $5.0 \times 10^6$  human V $\delta$ 2 T cells, 200  $\mu$ g/mouse anti-Tim-3 (Selleck, A2037), or their combination three times at five-day intervals. Human IgG4 was used as the isotype

control. Tumor volume (TV) was measured using a Vernier caliper to determine length (L) and width (W), and calculated as:  $TV = (L \times W^2)/2$ . Mice bearing tumors larger than 15 mm in any dimension were euthanized. All experiments were independently repeated three times. Animal protocols were approved by the Institutional Animal Care and Use Committee of Jinan University (approval number, IACUC-20230812–04).

#### Tumor infiltrating lymphocyte (TIL) analysis

Tumor tissues were sectioned and suspended in 15 mL of tumor digestion buffer containing 2% FBS, 1.5 mg/mL collagenase IV, and 10  $\mu$ g/mL DNase I. After rotating for 40 min at 37 °C, the cell suspension was filtered through a 100- $\mu$ m filter to obtain a single-cell suspension. TILs were isolated by density-gradient centrifugation using 50% and 70% Percoll (GE, 17,089,102). For intracellular staining, TILs were stimulated with 50 ng/mL PMA and 1  $\mu$ g/mL ionomycin in the presence of Golgi Stop for 4 h. They were then fixed and permeabilized with antibodies for 30 min at 4 °C in the dark, following the manufacturer's protocol. For surface staining, TILs were stained with the indicated antibodies and analyzed by full-spectrum flow cytometry.

#### Statistical analysis

Statistical analyses and graph generation were performed using GraphPad Prism (v.9). Data were obtained from independent biological samples and are presented as mean  $\pm$  standard deviation (SD).

## Results

#### Immune exhaustion markers were highly expressed on circulating T cells in NPC patients

We recruited 65 patients with NPC and 40 healthy donors (HD), analyzing the baseline expression of immune exhaustion and costimulatory markers on circulating CD4<sup>+</sup>, CD8<sup>+</sup>, V $\delta$ 2<sup>+</sup>, and V $\delta$ 1<sup>+</sup> T cells using flow cytometry (Fig. 1A; Supplementary Fig. 1A, B). Information on the characteristics of both HD and NPC patients is provided in Supplementary Table 1. The results showed that the percentages of circulating CD4<sup>+</sup> CD3<sup>+</sup> and CD28<sup>+</sup> CD8<sup>+</sup> T cells were significantly decreased, whereas

Tim-3<sup>+</sup> CD8<sup>+</sup>, Tim-3<sup>+</sup> CD4<sup>+</sup>, TIGIT<sup>+</sup> CD4<sup>+</sup> T cells were increased in NPC patients compared to healthy donors (Fig. 1B, C). Moreover, the percentages of innate-like circulating V $\delta$ 2<sup>+</sup> CD3<sup>+</sup> and CD28<sup>+</sup> V $\delta$ 1<sup>+</sup> T cells were significantly reduced, while the levels of PD-1<sup>+</sup> V $\delta$ 2<sup>+</sup>, Tim-3<sup>+</sup> V $\delta$ 2<sup>+</sup>, TIGIT<sup>+</sup> V $\delta$ 2<sup>+</sup>, PD-1<sup>+</sup> V $\delta$ 1<sup>+</sup>, Tim-3<sup>+</sup> V $\delta$ 1<sup>+</sup>, and TIGIT<sup>+</sup> V $\delta$ 1<sup>+</sup> T cell in NPC patients were significantly higher than those in healthy donors (Fig. 1D, E). To quantitatively assess the changes in immune parameters, we calculated the mean and logarithmic values of these parameters in NPC patients and HD. The results indicated that the proportion of circulating V $\delta$ 2<sup>+</sup> CD3<sup>+</sup> T cells was the most reduced in NPC, while Tim-3 on CD4<sup>+</sup>, CD8<sup>+</sup>, V $\delta$ 2<sup>+</sup>, and V $\delta$ 1<sup>+</sup> T cells was most elevated (Fig. 1F). Given that Epstein-Barr virus (EBV) infection is a major risk factor for NPC development [8], we next examined whether EBV infection was associated with increased levels of immune exhaustion markers on circulating T cells in NPC. Interestingly, we found that the percentage of PD-1<sup>+</sup> CD8<sup>+</sup> T cells in EBV+NPC patients was significantly higher than that in EBV- patients (Fig. 1G, H). Collectively, these results demonstrate that both the quantity and quality of innate-like circulating  $\gamma\delta$  T cells are diminished in NPC patients.

#### Low retinoic acid levels are associated with high Tim-3 expression in patients with NPC

We next examined the serum levels of RA using enzyme-linked immunosorbent assay (ELISA) and found that the serum levels of the bioactive form of RA in patients with NPC (stage II–IV) were significantly lower than those in healthy donors (Fig. 2A, B). Furthermore, RA levels in patients with NPC decreased as the disease progressed (Fig. 2C). Our findings also indicated that RA levels in EBV+NPC patients were not significantly different from those in EBV- patients (Fig. 2D). Notably, serum RA levels in NPC patients were negatively correlated with surface Tim-3 levels on circulating V $\delta$ 2<sup>+</sup> and CD8<sup>+</sup> T cells (Fig. 2E–J). Collectively, these data suggest that RA deficiency is linked to elevated Tim-3 levels on V $\delta$ 2<sup>+</sup> and CD8<sup>+</sup> T cells in NPC patients.

(See figure on next page.)

**Fig. 1** Immune exhaustion markers were highly expressed on circulating T cells in patients with NPC. **A** Flow cytometric analysis of immune exhaustion and costimulatory molecule expression on circulating T cells. Representative plots demonstrate the gating strategy (NPC). **B–E** Surface expression levels of PD-1, Tim-3, TIGIT, and CD28 on circulating  $\alpha\beta$  (CD4<sup>+</sup> and CD8<sup>+</sup>; HD,  $n=31$ ; NPC,  $n=65$ ) and  $\gamma\delta$  (V $\delta$ 2<sup>+</sup> and V $\delta$ 1<sup>+</sup>; HD,  $n=25$ –26; NPC,  $n=46$ –48) T cells in NPC and HD cohorts. **F** The relative expression of immune markers on circulating CD4<sup>+</sup>, CD8<sup>+</sup>, V $\delta$ 2<sup>+</sup>, and V $\delta$ 1<sup>+</sup> T cells was calculated as  $\text{Log}_2(\text{NPC}_{\text{mean}}/\text{HD}_{\text{mean}})$ . **G, H** Levels of exhaustion markers and costimulatory molecules on circulating  $\alpha\beta$  (CD4<sup>+</sup> and CD8<sup>+</sup>; EBV+,  $n=26$ ; EBV-,  $n=39$ ) and  $\gamma\delta$  (V $\delta$ 2<sup>+</sup> and V $\delta$ 1<sup>+</sup>; EBV+,  $n=17$ –18; EBV-,  $n=28$ –30) T cells in NPC (EBV positive, EBV+; EBV negative, EBV-). Data are presented mean  $\pm$  SD and were analyzed using a Two-tailed unpaired Student's *t*-test with Welch's correction or the Mann–Whitney *U* test. Significance was indicated as follows: \* $P < 0.05$ , \*\* $P < 0.01$ , \*\*\* $P < 0.001$ , \*\*\*\* $P < 0.0001$ , *n.s.*, not significant



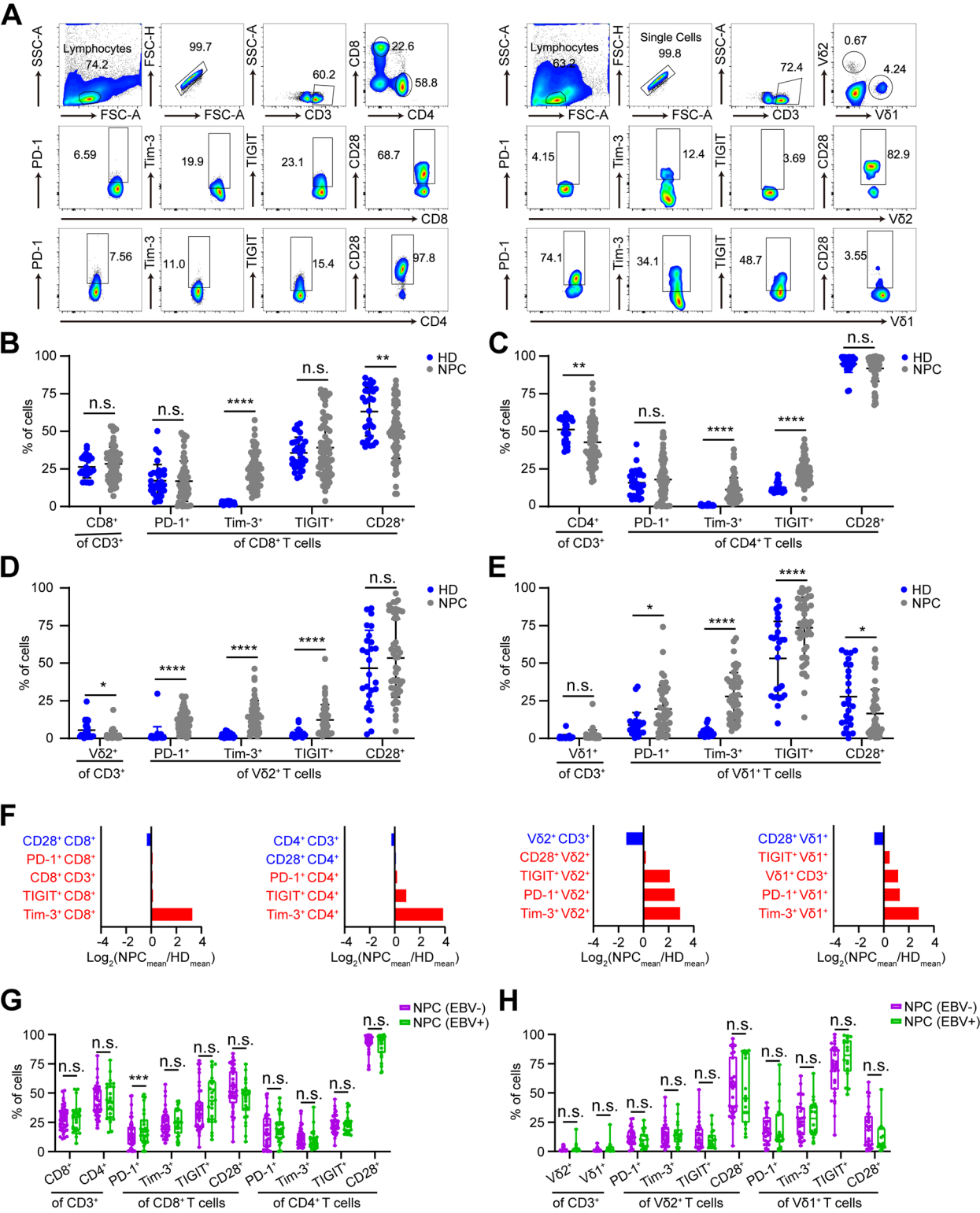


**Fig. 1** (See legend on previous page.)

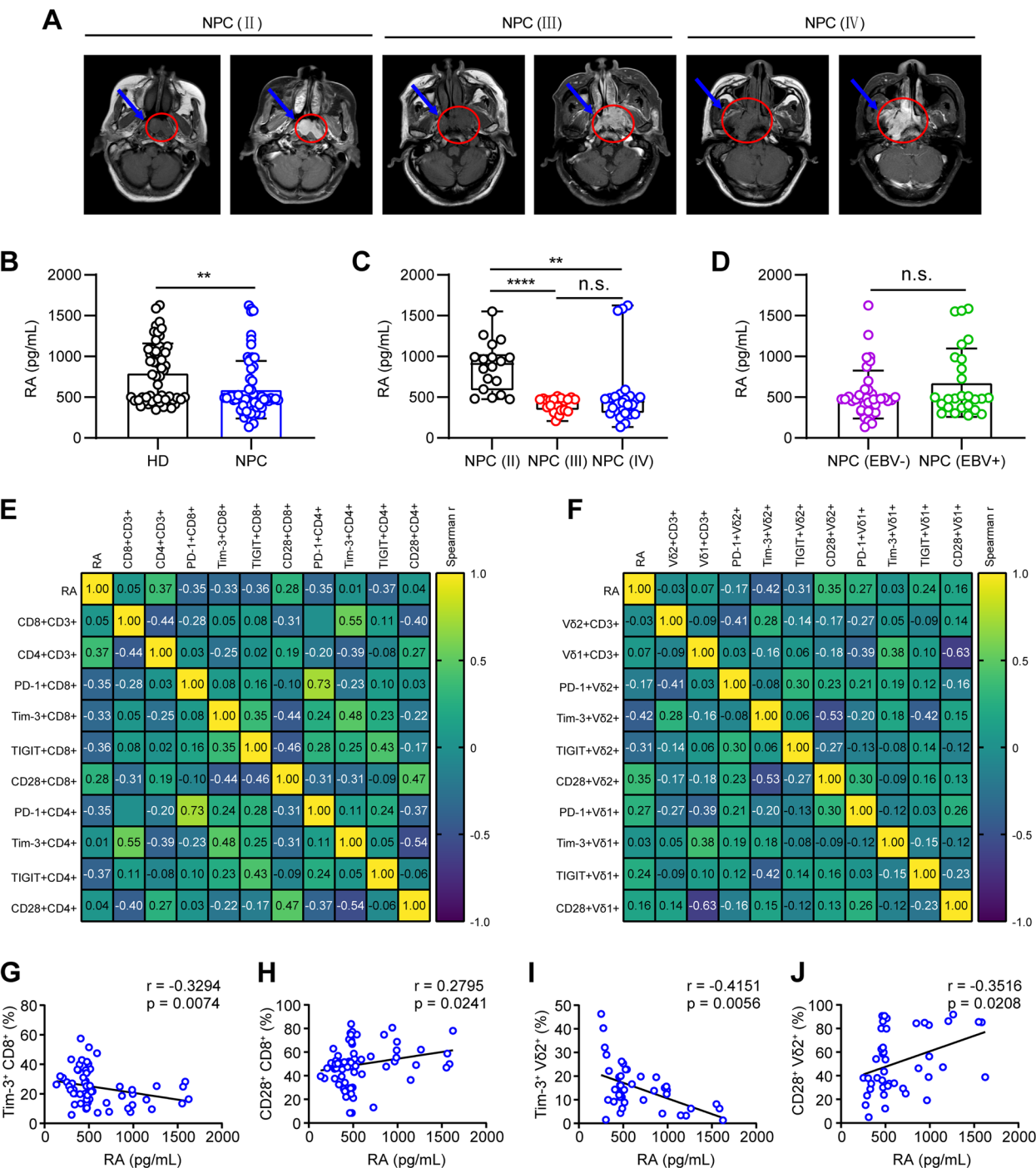


**Fig. 2** Low retinoic acid levels are associated with high Tim-3 expression in patients with NPC. **A** Magnetic resonance imaging (MRI) scans depicting tumor sizes in patients with primary NPC (II, III, and IV). **B** Serum RA levels in healthy donors (HD,  $n = 40$ ) and NPC ( $n = 65$ ) patients. **C** Graphical representation of RA levels in the serum of NPC patients stratified by stage (II,  $n = 18$ ; III,  $n = 21$ ; IV,  $n = 26$ ). **D** RA levels in NPC patients categorized by EBV status (EBV-,  $n = 39$ ; EBV+,  $n = 26$ ). **E, F** Correlations between RA levels and immune marker expression on circulating  $\alpha\beta$  ( $CD4^+$  and  $CD8^+$  T cells,  $n = 65$ ) and  $\gamma\delta$  T cells ( $V\delta1^+$  and  $V\delta2^+$  T cells,  $n = 43$ ). **G–J** Correlation analysis of Tim-3 and CD28 on circulating T cells ( $CD8$ ,  $n = 65$ ;  $V\delta2$ ,  $n = 43$ ) with RA levels in NPC patients. Two-tailed unpaired Student's  $t$ -test was employed in panels (**B** and **D**); while one-way ANOVA with Tukey's multiple comparison test was applied in panel (**C**). Spearman correlation coefficients were calculated for panels (**E–J**). Data are presented as the mean  $\pm$  SD. Significance was indicated as follows:  $*P < 0.05$ ,  $**P < 0.01$ ,  $***P < 0.001$ ,  $****P < 0.0001$ ,  $n.s.$ , not significant

### The RA/RAR signaling pathway alleviates immune exhaustion by reducing Tim-3 expression in $\gamma\delta$ T cells

To investigate the mechanism by which RA regulates immune exhaustion, we performed a transcriptomic analyses of V $\delta$ 2 T cells from healthy donors treated with RA or Vehicle. RA did not affect the purity of ZOL-expanded V $\delta$ 2 T cells in vitro (Supplementary Fig. 2A, B). The heatmap and chord plot demonstrated that RA reduced Tim-3 (*HAVCR2*) levels, while an increase in costimulatory molecular CD28 expression was observed in V $\delta$ 2 T cells (Fig. 3A, B). We observed that RA had no effect on the NKG2D expression of ZOL-expanded V $\delta$ 2 T cells in vitro (Fig. 3C, D). We found that treatment with RA for 24 h significantly inhibited the expression of Tim-3 in T cells, as determined by real-time quantitative PCR (Fig. 3E). The canonical action of retinoic acid involves binding to its receptors (RARs), which translocate to the nucleus and function as transcription factors [42]. However, Western blotting revealed that RA did not promote the expressions of RAR $\alpha$ , RAR $\beta$ , or RAR $\gamma$  in V $\delta$ 2 T cells (Supplementary Fig. 2C). Recently, Alexandre Larange et al. demonstrated that the RAR $\alpha$  receptor influences T cell receptor activation, thereby regulating the balance of immune responses [43]. Notably, RA treatment facilitated RAR $\alpha$  nuclear translocation in V $\delta$ 2 T cells (Fig. 3F). V $\delta$ 2 T cells expanded by zoledronic acid (ZOL) were treated with RA three times at one-day intervals. The results indicated that RA significantly decreased levels of TIGIT and Tim-3 while increasing CD28 expression in V $\delta$ 2 T cells (Fig. 3G, H; Supplementary Fig. 2D). To investigate how RA regulates the expression of immune exhaustion markers in V $\delta$ 2 T cells, we cultured V $\delta$ 2 T cells in the presence or absence of a RAR inhibitor (RARI, AGN194310), with or without RA treatment. We found that the inhibition of Tim-3 in response to RA was reversed by RARI treatment, whereas PD-1, TIGIT, and CD28 levels remained largely unchanged (Fig. 3I, J). Together, these results

reveal that RA/RAR signaling represses Tim-3 expression in V $\delta$ 2 T cells.

### RAR inhibitor attenuates RA-mediated NF- $\kappa$ B activation and decreases the expression of antitumor-related cytokines in V $\delta$ 2 T cells

To further elucidates how RA regulates cytotoxic T cells in antitumor responses, V $\delta$ 2 T cells from healthy donors were cultured for RNA-seq analysis. Differentially expressed genes (DEGs) were identified and subjected to KEGG pathway analysis (Fig. 4A). Notably, the TNF and T cell receptor signaling pathways were substantially activated after RA treatment (Fig. 4B-D). Indeed, RA/RAR mediated NF- $\kappa$ B activation in V $\delta$ 2 T-cells was confirmed by immunoblotting (Fig. 4E; Supplementary Fig. 3A, B). We hypothesized RA/RAR promotes antitumor cytokine production in these cells. To investigate whether the RA/RAR signaling pathway mediates cytokine production in V $\delta$ 2 T cells in vitro, the cells were treated with RA, RAR inhibitor (RARI), or their combination, followed by flow cytometry analysis. The results indicated that RA significantly promoted the levels of IFN- $\gamma$  and TNF- $\alpha$  in V $\delta$ 2 T cells, which were reversed by RARI treatment (Fig. 4F, G). Collectively, these findings demonstrate that RA/RAR signaling mediates NF- $\kappa$ B activation and enhances antitumor-related cytokine expression in human cytotoxic T cells.

### RA enhances antitumor immunity through $\gamma\delta$ T cells

To determine whether RA promotes antitumor immunity via RAR or  $\gamma\delta$  T cells, B16-F0 melanoma cells were inoculated subcutaneously into mice and treated with RA, RARI,  $\alpha$ TCR $\gamma/\delta$  antibody ( $\alpha$ TCR $\gamma/\delta$ ), or their combinations (Fig. 5A). The results showed that inhibition of RAR signaling in B16-F0 tumor-bearing mice diminished the antitumor effects of RA (Fig. 5B, C). Additionally, tumor-bearing mice were treated with anti-mouse TCR $\gamma/\delta$  antibody ( $\alpha$ TCR $\gamma/\delta$ ) to deplete  $\gamma\delta$  T cells under the therapy of RA, RARI, or their combination. Depletion of  $\gamma\delta$  T cells aggravated tumor growth and weakened

(See figure on next page.)

**Fig. 3** The RA/RAR signaling pathway alleviates immune exhaustion by reducing Tim-3 expression in  $\gamma\delta$  T cells. **A** RNA sequencing analysis of V $\delta$ 2 T cells pretreated with Vehicle (V) or RA ( $n=3$ ). **B** Chord diagram illustrating differentially expressed genes (DEGs) enriched in relevant signaling pathways. **C, D** V $\delta$ 2<sup>+</sup> T cells from healthy donors were treated with RA three times at 24-h intervals, followed by flow cytometric analysis (NKG2D<sup>+</sup> on V $\delta$ 2<sup>+</sup> T cells,  $n=4$ ). **E** mRNA levels of immune exhaustion markers in RA (12 h, 24 h, and 48 h) pretreated V $\delta$ 2<sup>+</sup> T cells were verified by Quantitative real-time PCR (qPCR), and their fold changes were shown in heat map (healthy donors,  $n=3$  per group). **F** Confocal imaging of RAR $\alpha$  (green) and nucleus (blue) in V $\delta$ 2 T cells treated with Vehicle or 250 nM RA for 12 h. **G, H** V $\delta$ 2<sup>+</sup> T cells from healthy donors were treated with RA three times at 24-h intervals, followed by flow cytometric analysis (PD-1<sup>+</sup>, Tim-3<sup>+</sup>, and TIGIT<sup>+</sup> on V $\delta$ 2<sup>+</sup> T cells,  $n=19$ ; CD28<sup>+</sup> on V $\delta$ 2<sup>+</sup> T cells,  $n=12$ ). **I, J** V $\delta$ 2 T cells were treated with vehicle, AGN194310 (RARI), RA, or combination for 24 h. Flow cytometric analysis and statistical evaluations of immune marker percentages are shown ( $n=16$ ). Two-tailed Unpaired Student's t-test (**D**), a paired Student's t-test was used in panel (**H**), and one-way ANOVA with Tukey's multiple comparisons test was used in panel (**J**). Data are presented as mean  $\pm$  SD. Significance was indicated as follows: \* $P<0.05$ , \*\* $P<0.01$ , \*\*\* $P<0.001$ , \*\*\*\* $P<0.0001$ , *n.s.*, not significant

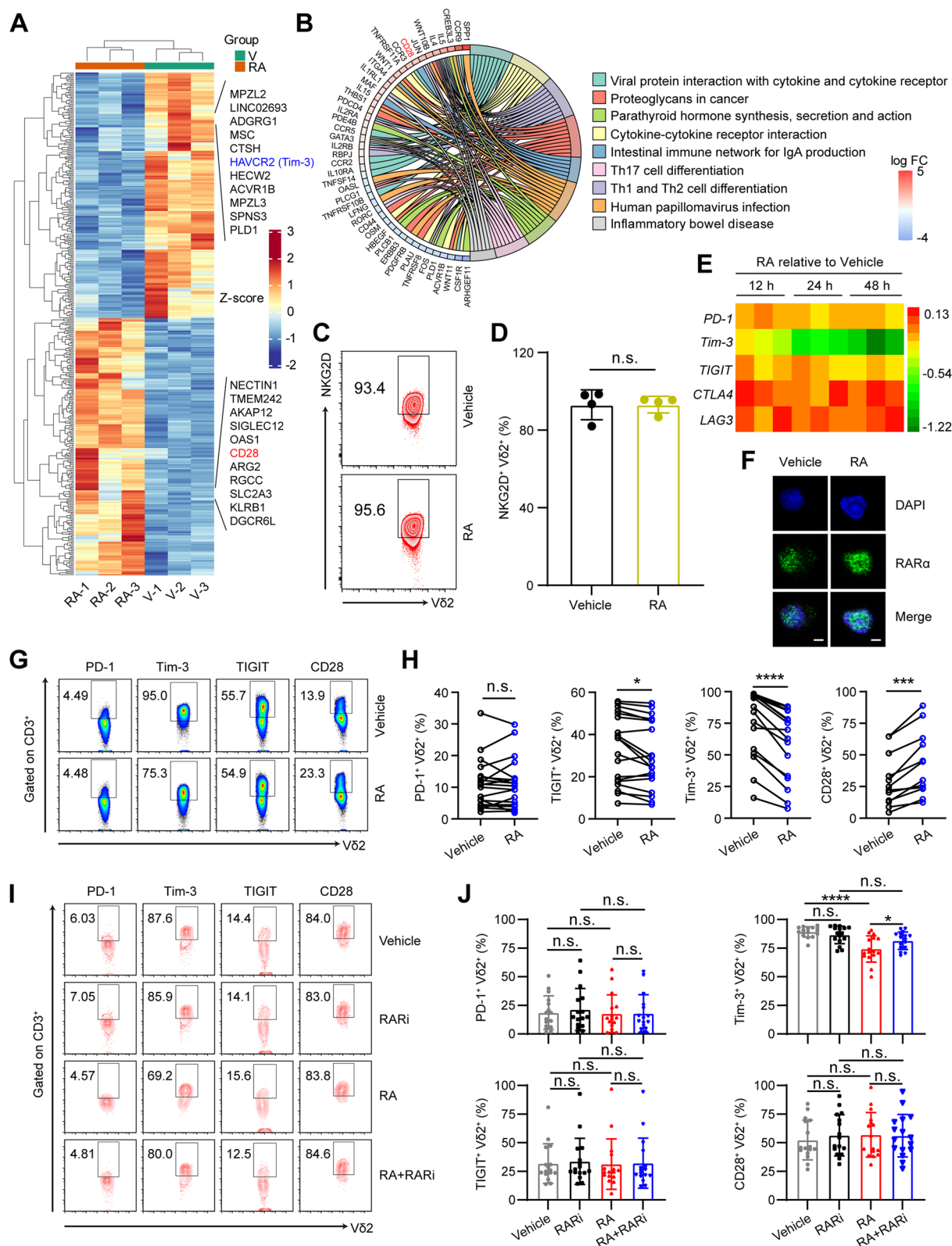


**Fig. 3** (See legend on previous page.)



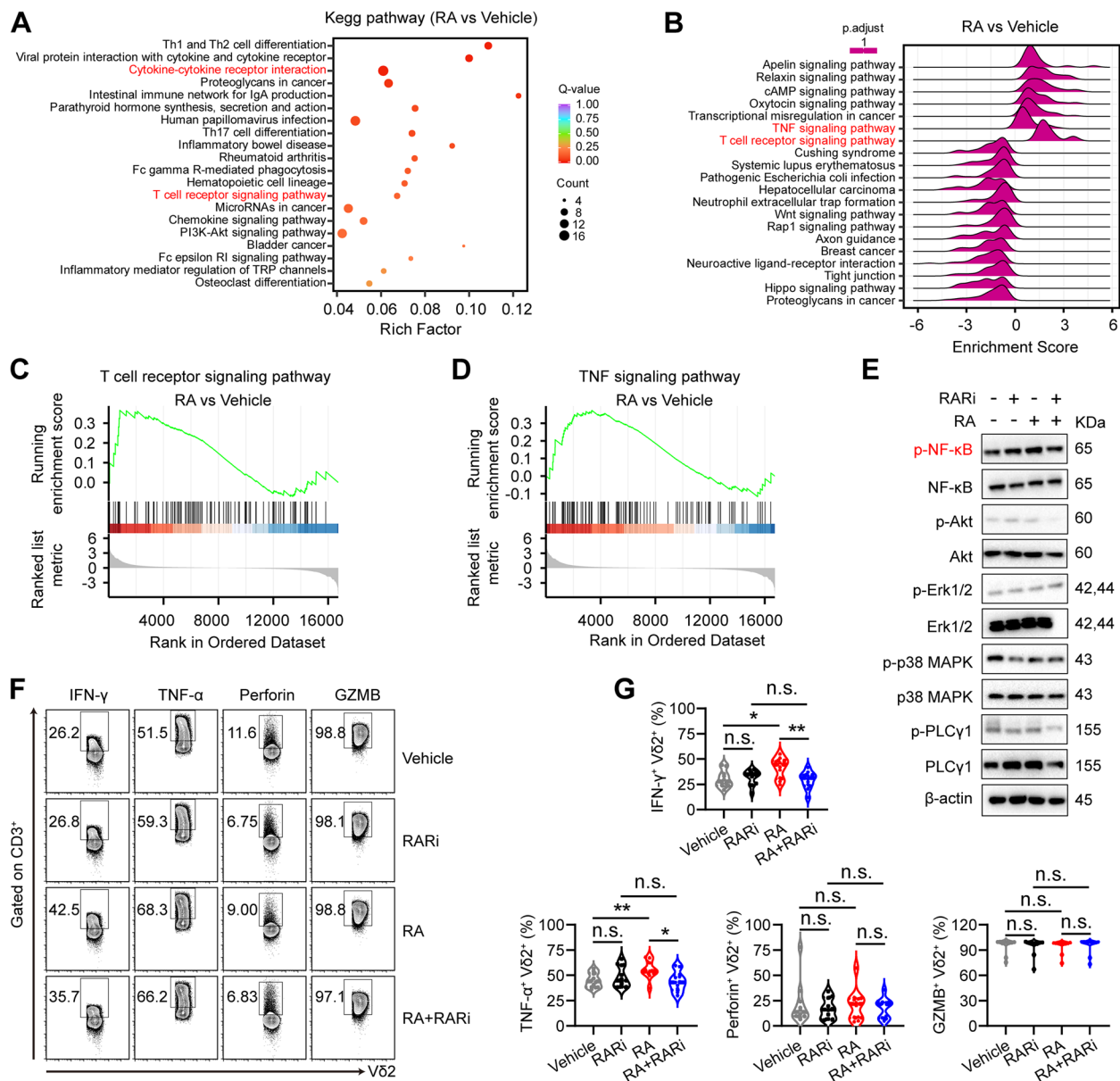


**Fig. 4** RAR inhibitor attenuates RA-mediated NF-κB activation and decreases the expression of antitumor-related cytokines in Vδ2 T cells. **A** RA- or vehicle-pretreated Vδ2 T cells were collected for RNA-seq analysis. The DEGs were analyzed using KEGG pathway enrichment analysis (RA vs Vehicle). **B** GSEA was performed for the top 20 signaling pathways. An enrichment score (ES) > 0 indicates that the pathway is activated, and an enrichment score < 0 indicates that the pathway is inhibited. **C, D** GSEA analysis was performed for the T-cell receptor signaling pathway (Enrichment Score = 0.36;  $p = 0.28$ ) and TNF signaling pathway (Enrichment Score = 0.37;  $p = 0.21$ ). **E** Vδ2 T cells were treated with vehicle, RARi, RA, or their combination for 24 h, activated with phorbol 12-myristate 13-acetate (PMA) and ionomycin (Ion) for another 2 h, and then harvested for immunoblot analysis. **F, G** Vδ2 T cells were stimulated with vehicle, RARi, RA, or their combination for 24 h, followed by activation with PMA Ion for another 4 h under the condition of Golgi-Plug, and then harvested for flow cytometry analysis ( $n = 10$ ). One-way ANOVA with Tukey's multiple comparison test (**G**). Data are represented as the mean  $\pm$  SD. \* $P < 0.05$ , \*\* $P < 0.01$ , \*\*\* $P < 0.001$ , \*\*\*\* $P < 0.0001$ , n.s., not significant

RA-mediated antitumor immunity (Fig. 5D; Supplementary Fig. 4A). Interestingly, administration of RA significantly improved survival in tumor-bearing mice, with the effects being dependent on both RAR signaling and  $\gamma\delta$  T cells (Fig. 5E). Further investigation revealed that RA/

RAR signaling promoted the antitumor immunity of  $\gamma\delta$  T cells in vivo. The inhibition of exhaustion markers PD-1 and Tim-3 on tumor-infiltrating  $\gamma\delta$  T cells by RA was reversed by RARi, although the percentage of tumor-infiltrating  $\gamma\delta$  T cells was not affected by RA/RAR signaling

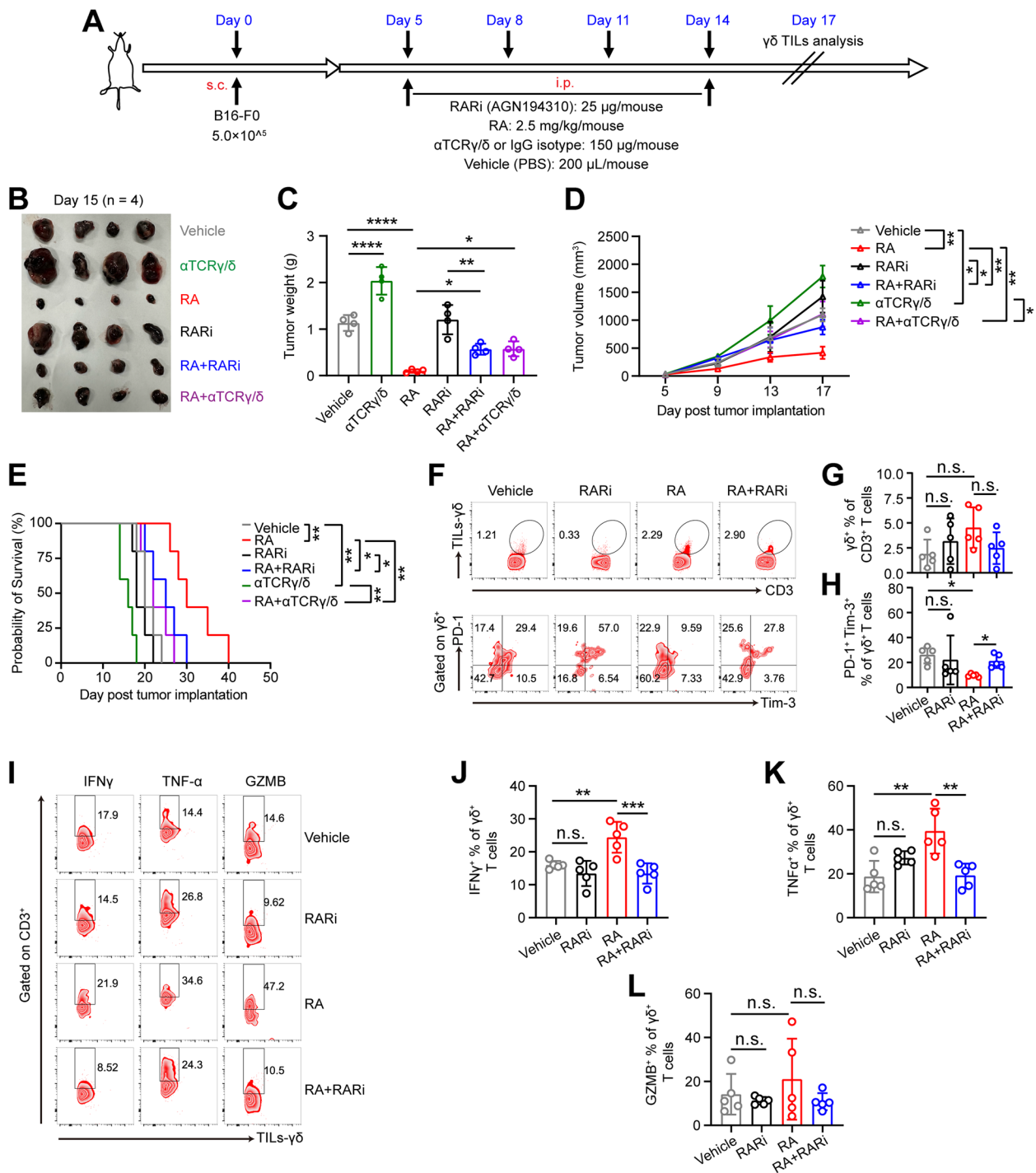


**Fig. 5** RA reverses immune exhaustion and promotes antitumor immunity of  $\gamma\delta$  T cells. **A** Experimental design: Mice were inoculated with B16-F0 tumor cells, followed by the specified treatment. Wild-type mice received B16-F0 tumor inoculation, followed by treatment with RA, RARi,  $\alpha\text{TCR}\gamma/\delta$  (anti-TCR $\gamma/\delta$ ) either as monotherapy or combination therapy. Each experiment was independently repeated three times. **B** Representative images of B16-F0 tumors from mice on day 15 post-tumor implantation (n = 4 per group). **C** Tumor weight of mice in each group at the end of the experiment (n = 4 per group). **D**, **E** Tumor growth (**D**) and survival curves (**E**) in mice treated with RA, RARi,  $\alpha\text{TCR}\gamma/\delta$  alone or in combination (n = 5 per group). **F–H** Exhaustion marker expression on tumor-infiltrating lymphocytes (TILs) was analyzed by flow cytometry (**F–H**). **I–L** Levels of IFN- $\gamma$ , TNF- $\alpha$ , and Granzyme B (GZMB) in TILs- $\gamma\delta$  T cells after RA or RARi treatment, alone or in combination (n = 5 per group). Each experiment was independently repeated three times. One-way ANOVA with Tukey's multiple comparisons test was used for panels (**C**, **D**, **J**, **K**, and **L**); the log-rank (Mantel-Cox) test was used for panel (**E**). Data are presented as mean  $\pm$  SD. \* $P < 0.05$ , \*\* $P < 0.01$ , \*\*\* $P < 0.001$ , \*\*\*\* $P < 0.0001$ , n.s., not significant

(Fig. 5F–H; Supplementary Fig. 4B). Moreover, RA treatment increased the percentage of IFN- $\gamma$  and TNF- $\alpha$  in tumor infiltrating  $\gamma\delta$  T cells, which was mitigated by RAR inhibitor (Fig. 5I–L). Interestingly, RA-mediated antitumor immunity was also partially dependent on CD8 T cells (Supplementary Fig. 5A–C). These findings suggest that RA alleviates immune exhaustion and enhances the antitumor activity of  $\gamma\delta$  T cells in vivo.

#### RA improves V $\delta$ 2 T cell-mediated immunotherapy efficacy in human NPC by suppressing Tim-3 expression

To determine whether RA improves antitumor immunity by modulating Tim-3 expression on human V $\delta$ 2 T cells, C666-1 nasopharyngeal carcinoma cells were inoculated subcutaneously into M-NSG mice, followed by treatment with RA,  $\alpha$ TIM-3 antibody, V $\delta$ 2 T cells, or their combinations (Fig. 6A). The levels Tim-3 on V $\delta$ 2 T cells treated with either  $\alpha$ TIM-3 or RA were significantly lower than those in the control group (Supplementary Fig. 6A, B). To validate whether RA enhanced the therapeutic efficacy of V $\delta$ 2 T cells, we conducted an in vitro tumor-killing assay. The results preliminarily demonstrated that RA improved the antitumor immune response of V $\delta$ 2 T cells in vitro (Fig. 6B, C). Importantly, hematoxylin–eosin (H & E) staining showed no tissue injury following treatment with V $\delta$ 2 T cells ( $\gamma\delta$ -T), V $\delta$ 2+RA ( $\gamma\delta$ -T+RA), or V $\delta$ 2+ $\alpha$ TIM-3 ( $\gamma\delta$ -T+ $\alpha$ TIM-3), either alone or in combination (Fig. 6D). Notably, the combination of V $\delta$ 2 T cells with either RA or  $\alpha$ TIM-3 resulted in more pronounced tumor regression than either treatment alone (Fig. 6E, F). However, no significant difference in tumor volume reduction was observed between the combination treatments and V $\delta$ 2 T cells with RA/ $\alpha$ TIM-3 alone at day 36 in the C666-1 tumor-bearing mouse model (Fig. 6G). Nevertheless, the survival curve indicated improved survival in mice treated with the combination of V $\delta$ 2 T cells and RA or  $\alpha$ TIM-3 (Fig. 6H). To further elucidate the role of RAR in antitumor immunity, CRISPR-Cas9 technology was used to generate RAR $\alpha$  knockout V $\delta$ 2 T cells,

and immunoblotting confirmed the knockout efficiency (Fig. 6I, J; Supplementary Table 2). We observed that RA supplementation alleviated V $\delta$ 2 T cell immune exhaustion and enhanced antitumor immune activity. However, following RAR $\alpha$  knockout, RA supplementation failed to effectively alleviate immune exhaustion or augment antitumor immune responses (Fig. 6K–N). RAR $\alpha$  knockout V $\delta$ 2 T cells pretreated with RA,  $\alpha$ Tim-3, or vehicle were co-cultured with C666-1 tumor cells for 6 or 12 h, and tumor lysis was measured via LDH release. Our results further demonstrated that the antitumor activity of RAR $\alpha$  knockout V $\delta$ 2 T cells was partially reduced, but RA or  $\alpha$ Tim-3 supplementation improved  $\gamma\delta$  T cell cytotoxicity against nasopharyngeal carcinoma cells (Fig. 6O; Supplementary Fig. 6C). Collectively, these findings suggest that RA or  $\alpha$ TIM-3 improves the therapeutic efficacy of  $\gamma\delta$  T cells in nasopharyngeal carcinoma tumor-bearing mice.

#### Discussion

T cell exhaustion, characterized by elevated levels of immune inhibitory receptors within the tumor microenvironment (TME), remains a critical factor contributing to tumor immune evasion [14, 44]. Immunotherapies targeting multiple immune checkpoint receptors, including PD-1 and PD-L1 monoclonal antibodies, have demonstrated considerable success across various cancer patients [14, 45, 46]. However, solely employing antibody blockade therapies presents challenges in reversing T cell exhaustion intrinsically.

Recent studies have highlighted the potential role of nutrients, particularly vitamins, in alleviating cytotoxic T cell exhaustion and enhancing both antitumor and antiviral immune responses in the TME [12, 47]. Among these, vitamin D has shown promise; however, the specific effects of vitamin A on innate-like  $\gamma\delta$  T cell biology remain inadequately understood. Larange et al. recently underscored the importance of subcellular retinoic acid (RA)/RAR $\alpha$  signaling in T cells, identifying extranuclear

(See figure on next page.)

**Fig. 6** RA and RAR signaling improve V $\delta$ 2 T cell-mediated immunotherapy efficacy in human NPC by suppressing Tim-3 expression. **A** Overview of study design. M-NSG mice were inoculated with C666-1 tumor cells, followed by the indicated treatments. **B, C** V $\delta$ 2 T cells were pre-treated with RA or vehicle, incubated with MCF-7 or Jurkat tumor cells for 12 h, and cytotoxic efficiency was assessed via LDH release ( $n=3$ ). **D** Tissue pathology of the specified organs was assessed by hematoxylin and eosin staining on day 31 post-tumor implantation. **E** Images of C666-1 tumors in mice at day 31 post-tumor implantation ( $n=4$  per group). Each experiments were independently repeated three times. **F** Tumor weight ( $n=5$  per group). **G, H** Tumor volume (**G**) and survival curves (**H**) of mice treated with IgG, RA, V $\delta$ 2 T cells alone, or in combination with  $\alpha$ Tim-3 ( $n=5$  per group). **I, J** V $\delta$ 2 T cells were transfected with either an RAR $\alpha$  knockout vector (gRNA S1 targeting RAR $\alpha$ ) or a control vector (NC), followed by RA treatment twice at 1-day intervals. Protein levels were analyzed by immunoblotting (**I**) and quantified using Image J software (**J**). **K–N** Immune markers and cytokine levels were assessed by flow cytometry ( $n=3$  per group). **O** RAR $\alpha$  knockout or control (NC) V $\delta$ 2 T cells were treated with RA or  $\alpha$ Tim-3, incubated with C666-1 tumor cells for 12 h, and cytotoxic efficiency was assessed via LDH release ( $n=3$ ). Two-tailed unpaired Student's t-test was used in panel (**J**); one-way ANOVA with Tukey's multiple comparisons test was used for panels (**B, C, F, G, L, N, and O**); the log-rank (Mantel-Cox) test was used in panel (**H**). Data are presented as mean  $\pm$  SD. \* $P<0.05$ , \*\* $P<0.01$ , \*\*\* $P<0.001$ , \*\*\*\* $P<0.0001$ , n.s., not significant

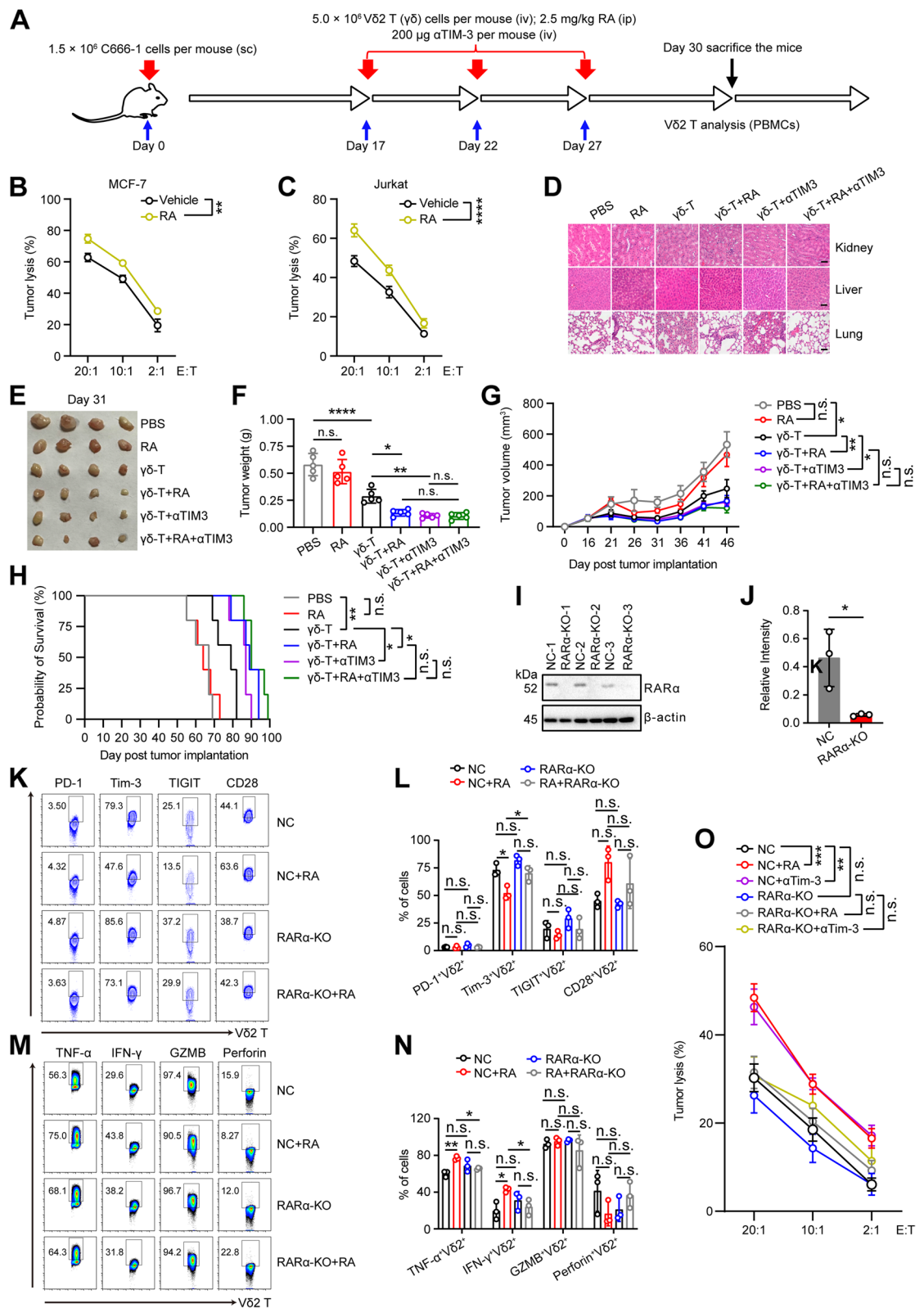


**Fig. 6** (See legend on previous page.)



RAR $\alpha$  as a component of the T cell receptor signalosome, essential for immune responses [43]. Our findings indicate that RA mitigates  $\gamma\delta$  T cell exhaustion through RAR signaling, thereby improving antitumor responses.

Previous research has demonstrated enhanced antitumor immunity in mice fed a vitamin A acetate-enriched diet [48]. Furthermore, Guo et al. illustrated that RA/RAR signaling augments antitumor efficacy via CD8<sup>+</sup> T cells, underscoring the pivotal role of adaptive immune cells, particularly cytotoxic CD8<sup>+</sup> T cells, in tumor immunity [33, 39]. Additionally, Ross and Raverdeau et al. reviewed how RA signaling modulates the proliferation, differentiation, and activation of immune cells, including dendritic cells (DCs), macrophages, natural killer (NK) cells, B cells, and T cells [36, 42, 49, 50]. Despite these advances, the precise mechanisms by which RA and its receptors regulate immune exhaustion, and their potential to enhance  $\gamma\delta$  T cell-mediated therapeutic efficacy, remain poorly understood.

RA binds to retinoic acid receptors (RARs), triggering their nuclear translocation and subsequent regulation of gene transcription [36, 39, 42]. Notably, prolonged RA treatment markedly reduced the expression of inhibitory receptors TIGIT and Tim-3 while increasing the levels of the costimulatory molecule CD28 on V $\delta$ 2 T cells. Moreover, RA/RAR signaling reduced Tim-3 expression and enhanced the production of IFN- $\gamma$  and TNF- $\alpha$  in cytotoxic V $\delta$ 2 T cells, leading to improved immunotherapeutic efficacy in a nasopharyngeal carcinoma (NPC) animal model. Nevertheless, further research is needed to elucidate how different RAR subtypes—specifically RAR $\alpha$ , RAR $\beta$ , and RAR $\gamma$ —modulate immune exhaustion and cytokine production associated with antitumor activity.

## Conclusion

In summary, our clinical data revealed that serum RA levels in NPC patients were significantly lower than those in healthy controls, and markers of immune exhaustion were highly expressed on circulating  $\gamma\delta$  T cells. Correlation analysis demonstrated that low serum retinoic acid levels were associated with elevated Tim-3 levels in NPC patients. Importantly, RA/RAR signaling reversed immune exhaustion and enhanced the immunotherapeutic efficacy of  $\gamma\delta$  T cells both *in vitro* and *in vivo*. Collectively, RA and RAR-targeted therapies present a safe and cost-effective approach with broad potential to improve antitumor responses in cancer patients.

## Supplementary Information

The online version contains supplementary material available at <https://doi.org/10.1186/s12964-025-02161-8>.

Supplementary Material 1.

Supplementary Material 2.

## Acknowledgements

The authors would like to thank all the colleagues who contributed to this study.

## Authors' contributions

PL, LL, and JZ conceived of the project and designed the study. GL, QQ, XZ, DZ, GZ, and PL performed the experiments and acquired data. GL, PL, HD, and JZ drafted the manuscript. LPan, QQ, KL, and LP provided technical assistance. GL and PL analyzed and interpreted the data. GL, PL, and JZ contributed to manuscript preparation.

## Funding

This work is supported by the National Natural Science Foundation of China (grant 32300728 to P.L.), the Guangdong Basic and Applied Basic Research Foundation (grant 2022A1515110416 to P.L.), and the 14th Five-Year high level key specialty of FoShan City.

## Data availability

The raw sequence data reported in this paper have been deposited in the Genome Sequence Archive (Genomics, Proteomics & Bioinformatics 2021) in National Genomics Data Center (Nucleic Acids Res 2022), China National Center for Bioinformation / Beijing Institute of Genomics, Chinese Academy of Sciences (GSA-Human: HRA006920) that are publicly accessible at <https://ngdc.cncb.ac.cn/gsa-human>. All data supporting the findings of this study are presented in the paper. Further inquiries can be directed to the corresponding author.

## Declarations

### Ethics approval and consent to participate

This study was approved by the Institutional Review Board of the First People's Hospital of Foshan, Foshan, P. R. China (approval number, FSYYY-EC-SOP-008-02.0-A09). Animal protocols were approved by the Institutional Animal Care and Use Committee of Jinan University (approval number, IACUC-20230812-04).

### Competing interests

The authors declare no competing interests.

Received: 10 November 2024 Accepted: 19 March 2025

Published online: 29 March 2025

## References

- Lin M, Zhang XL, You R, Liu YP, Cai HM, Liu LZ, Liu XF, Zou X, Xie YL, Zou RH, et al. Evolutionary route of nasopharyngeal carcinoma metastasis and its clinical significance. *Nat Commun*. 2023;14:610.
- Jin S, Li R, Chen MY, Yu C, Tang LQ, Liu YM, Li JP, Liu YN, Luo YL, Zhao Y, et al. Single-cell transcriptomic analysis defines the interplay between tumor cells, viral infection, and the microenvironment in nasopharyngeal carcinoma. *Cell Res*. 2020;30:950–65.
- Ding X, Hua YJ, Zou X, Chen XZ, Zhang XM, Xu B, Ouyang YF, Tu ZW, Li HF, Duan CY, et al. Camrelizumab plus famitinib in patients with recurrent or metastatic nasopharyngeal carcinoma treated with PD-1 blockade: data from a multicohort phase 2 study. *EClinicalMedicine*. 2023;61: 102043.
- Liang Y, Li J, Li Q, Tang L, Chen L, Mao Y, He Q, Yang X, Lei Y, Hong X, et al. Plasma protein-based signature predicts distant metastasis and induction chemotherapy benefit in Nasopharyngeal Carcinoma. *Theranostics*. 2020;10:9767–78.
- Ding RB, Chen P, Rajendran BK, Lyu X, Wang H, Bao J, Zeng J, Hao W, Sun H, Wong AH, et al. Molecular landscape and subtype-specific therapeutic response of nasopharyngeal carcinoma revealed by integrative pharmacogenomics. *Nat Commun*. 2021;12:3046.

6. Liu Y, Lui KS, Ye Z, Fung TY, Chen L, Sit PY, Leung CY, Mak NK, Wong KL, Lung HL, et al. EBV latent membrane protein 1 augments gammadelta T cell cytotoxicity against nasopharyngeal carcinoma by induction of butyrophilin molecules. *Theranostics*. 2023;13:458–71.
7. Wang G, Mudgal P, Wang L, Shuen TWH, Wu H, Alexander PB, Wang WW, Wan Y, Toh HC, Wang XF, Li QJ. TCR repertoire characteristics predict clinical response to adoptive CTL therapy against nasopharyngeal carcinoma. *Oncoimmunology*. 2021;10:1955545.
8. Chen YP, Chan ATC, Le QT, Blanchard P, Sun Y, Ma J. Nasopharyngeal carcinoma. *Lancet*. 2019;394:64–80.
9. Wang X, Zhang Y, Mu X, Tu CR, Chung Y, Tsao SW, Chan GC, Leung WH, Lau YL, Liu Y, Tu W. Exosomes derived from gammadelta-T cells synergize with radiotherapy and preserve antitumor activities against nasopharyngeal carcinoma in immunosuppressive microenvironment. *J Immunother Cancer*. 2022;10:e003832.
10. Zhao JJ, Zhou S, Chen CL, Zhang HX, Zhou ZQ, Wu ZR, Liu Y, Pan QZ, Zhu Q, Tang Y, et al. Clinical Effect of Adjuvant Cytokine-Induced Killer Cells Immunotherapy in Patients with Stage II-IVB Nasopharyngeal Carcinoma after Chemoradiotherapy: A propensity score analysis. *J Cancer*. 2018;9:4204–14.
11. Teo PM, Kwan WH, Lee WY, Leung SF, Johnson PJ. Prognosticators determining survival subsequent to distant metastasis from nasopharyngeal carcinoma. *Cancer*. 1996;77:2423–31.
12. Li P, Zhu X, Cao G, Wu R, Li K, Yuan W, Chen B, Sun G, Xia X, Zhang H, et al. 1alpha,25(OH)2D3 reverses exhaustion and enhances antitumor immunity of human cytotoxic T cells. *J Immunother Cancer*. 2022;10:e003477.
13. Galon J, Bruni D. Tumor Immunology and Tumor Evolution: Intertwined Histories. *Immunity*. 2020;52:55–81.
14. Chow A, Perica K, Klebanoff CA, Wolchok JD. Clinical implications of T cell exhaustion for cancer immunotherapy. *Nat Rev Clin Oncol*. 2022;19:775.
15. Mensurado S, Blanco-Dominguez R, Silva-Santos B. The emerging roles of gammadelta T cells in cancer immunotherapy. *Nat Rev Clin Oncol*. 2023;20:178–91.
16. Serrano R, Lettau M, Zarobkiewicz M, Wesch D, Peters C, Kabelitz D. Stimulatory and inhibitory activity of STING ligands on tumor-reactive human gamma/delta T cells. *Oncoimmunology*. 2022;11:2030021.
17. Sebestyen Z, Prinz I, Dechanet-Merville J, Silva-Santos B, Kuball J. Translating gammadelta (gammadelta) T cells and their receptors into cancer cell therapies. *Nat Rev Drug Discov*. 2020;19:169–84.
18. Li P, Wu R, Li K, Yuan W, Zeng C, Zhang Y, Wang X, Zhu X, Zhou J, Li P, Gao Y. IDO Inhibition Facilitates Antitumor Immunity of Vgamma9Vdelta2 T Cells in Triple-Negative Breast Cancer. *Front Oncol*. 2021;11:679517.
19. Li P, Li K, Yuan W, Xu Y, Li P, Wu R, Han J, Yin Z, Lu L, Gao Y. 1alpha,25(OH)2D3 ameliorates insulin resistance by alleviating gammadelta T cell inflammation via enhancing fructose-1,6-bisphosphatase 1 expression. *Theranostics*. 2023;13:5290–304.
20. Gentles AJ, Newman AM, Liu CL, Bratman SV, Feng W, Kim D, Nair VS, Xu Y, Khuong A, Hoang CD, et al. The prognostic landscape of genes and infiltrating immune cells across human cancers. *Nat Med*. 2015;21:938–45.
21. Xu Y, Xiang Z, Alnaggar M, Kouakanou L, Li J, He J, Yang J, Hu Y, Chen Y, Lin L, et al. Allogeneic Vgamma9Vdelta2 T-cell immunotherapy exhibits promising clinical safety and prolongs the survival of patients with late-stage lung or liver cancer. *Cell Mol Immunol*. 2021;18:427–39.
22. Silva-Santos B, Mensurado S, Coffelt SB. gammadelta T cells: pleiotropic immune effectors with therapeutic potential in cancer. *Nat Rev Cancer*. 2019;19:392–404.
23. Zhang X, Zhang C, Qiao M, Cheng C, Tang N, Lu S, Sun W, Xu B, Cao Y, Wei X, et al. Depletion of BATF in CAR-T cells enhances antitumor activity by inducing resistance against exhaustion and formation of central memory cells. *Cancer Cell*. 2022;40:1407.
24. Roe K. NK-cell exhaustion, B-cell exhaustion and T-cell exhaustion-the differences and similarities. *Immunology*. 2022;166:155–68.
25. Daniel B, Yost KE, Hsiung S, Sandoz K, Xia Y, Qi Y, Hiam-Galvez KJ, Black M, Raposo CJ, Shi Q, et al. Divergent clonal differentiation trajectories of T cell exhaustion. *Nat Immunol*. 2022;23:1614.
26. Fucikova J, Rakova J, Hensler M, Kasikova L, Belicova L, Hladikova K, Truxova I, Skapa P, Laco J, Pecan L, et al. TIM-3 Dictates Functional Orientation of the Immune Infiltrate in Ovarian Cancer. *Clin Cancer Res*. 2019;25:4820–31.
27. Ausejo-Mauleon I, Labiano S, de la Nava D, Laspidea V, Zalacain M, Marrocan L, Garcia-Moure M, Gonzalez-Huarriz M, Hervas-Corpcion I, Dhandapani L, et al. TIM-3 blockade in diffuse intrinsic pontine glioma models promotes tumor regression and antitumor immune memory. *Cancer Cell*. 1911;2023:41.
28. Zheng S, Song J, Linghu D, Yang R, Liu B, Xue Z, Chen Q, Liu C, Zhong D, Hung MC, Sun L. Galectin-9 blockade synergizes with ATM inhibition to induce potent anti-tumor immunity. *Int J Biol Sci*. 2023;19:981–93.
29. Rudloff MW, Zumbo P, Favret NR, Roetman JJ, Detres Roman CR, Erwin MM, Murray KA, Jonnakuti ST, Dundar F, Betel D, Philip M. Hallmarks of CD8(+) T cell dysfunction are established within hours of tumor antigen encounter before cell division. *Nat Immunol*. 2023;24:1527.
30. Galluzzi L, Aryankalayil MJ, Coleman CN, Formenti SC. Emerging evidence for adapting radiotherapy to immunotherapy. *Nat Rev Clin Oncol*. 2023;20:543–57.
31. Weber EW, Parker KR, Sotillo E, Lynn RC, Anbunathan H, Lattin J, Good Z, Belk JA, Daniel B, Klysz D, et al. Transient rest restores functionality in exhausted CAR-T cells through epigenetic remodeling. *Science*. 2021;372:eaba1786.
32. Mora JR, Iwata M, von Andrian UH. Vitamin effects on the immune system: vitamins A and D take centre stage. *Nat Rev Immunol*. 2008;8:685–98.
33. Guo Y, Pino-Lagos K, Ahonen CA, Bennett KA, Wang J, Napoli JL, Blomhoff R, Sockanathan S, Chandraratna RA, Dmitrovsky E, et al. A retinoic acid-rich tumor microenvironment provides clonal survival cues for tumor-specific CD8(+) T cells. *Cancer Res*. 2012;72:5230–9.
34. Mirza N, Fishman M, Fricke I, Dunn M, Neuger AM, Frost TJ, Lush RM, Antonia S, Gabrilovich DI. All-trans-retinoic acid improves differentiation of myeloid cells and immune response in cancer patients. *Cancer Res*. 2006;66:9299–307.
35. Hong Y, Manoharan I, Suryawanshi A, Majumdar T, Angus-Hill ML, Koni PA, Manicassamy B, Mellor AL, Munn DH, Manicassamy S. beta-catenin promotes regulatory T-cell responses in tumors by inducing vitamin A metabolism in dendritic cells. *Cancer Res*. 2015;75:656–65.
36. Ross AC. Vitamin A and retinoic acid in T cell-related immunity. *Am J Clin Nutr*. 2012;96:1166S–1172S.
37. Tobin RP, Cogswell DT, Cates VM, Davis DM, Borgers JSW, Van Gulick RJ, Katsnelson E, Coutts KL, Jordan KR, Gao D, et al. Targeting MDSC Differentiation Using ATRA: A Phase I/II Clinical Trial Combining Pembrolizumab and All-Trans Retinoic Acid for Metastatic Melanoma. *Clin Cancer Res*. 2023;29:1209–19.
38. Peng Z, Wang J, Guo J, Li X, Wang S, Xie Y, Jiang H, Wang Y, Wang M, Hu M, et al. All-trans retinoic acid improves NSD2-mediated RARalpha phase separation and efficacy of anti-CD38 CAR-T-cell therapy in multiple myeloma. *J Immunother Cancer*. 2023;11:e006325.
39. Guo Y, Nolle RJ. Retinoic acid on stage in antitumor immunity. *Oncoimmunology*. 2013;2:e22985.
40. Rao E, Hou Y, Huang X, Wang L, Wang J, Zheng W, Yang H, Yu X, Yang K, Bugno J, et al. All-trans retinoic acid overcomes solid tumor radioresistance by inducing inflammatory macrophages. *Sci Immunol*. 2021;6:eaba8426.
41. Zhu X, Li K, Liu G, Wu R, Zhang Y, Wang S, Xu M, Lu L, Li P. Microbial metabolite butyrate promotes anti-PD-1 antitumor efficacy by modulating T cell receptor signaling of cytotoxic CD8 T cell. *Gut Microbes*. 2023;15:2249143.
42. Raverdeau M, Mills KH. Modulation of T cell and innate immune responses by retinoic acid. *J Immunol*. 2014;192:2953–8.
43. Larange A, Takazawa I, Kakugawa K, Thiault N, Ngoi S, Olive ME, Iwaya H, Seguin L, Vicente-Suarez I, Becart S, et al. A regulatory circuit controlled by extranuclear and nuclear retinoic acid receptor alpha determines T cell activation and function. *Immunity*. 2023;56(2054–2069): e2010.
44. Jhunjunwala S, Hammer C, Delamarre L. Antigen presentation in cancer: insights into tumour immunogenicity and immune evasion. *Nat Rev Cancer*. 2021;21:298–312.
45. Kraehenbuehl L, Weng CH, Eghbali S, Wolchok JD, Merghoub T. Enhancing immunotherapy in cancer by targeting emerging immunomodulatory pathways. *Nat Rev Clin Oncol*. 2022;19:37–50.
46. Galluzzi L, Humeau J, Buque A, Zitvogel L, Kroemer G. Immunostimulation with chemotherapy in the era of immune checkpoint inhibitors. *Nat Rev Clin Oncol*. 2020;17:725–41.
47. Li K, Lu E, Wang Q, Xu R, Yuan W, Wu R, Lu L, Li P. Serum vitamin D deficiency is associated with increased risk of gammadelta T cell exhaustion in HBV-infected patients. *Immunology*. 2024;171:31–44.

48. Malkovsky M, Dore C, Hunt R, Palmer L, Chandler P, Medawar PB. Enhancement of specific antitumor immunity in mice fed a diet enriched in vitamin A acetate. *Proc Natl Acad Sci U S A*. 1983;80:6322–6.
49. Herberman RB, Ortaldo JR. Natural killer cells: their roles in defenses against disease. *Science*. 1981;214:24–30.
50. Goldfarb RH, Herberman RB. Natural killer cell reactivity: regulatory interactions and among phorbol ester, interferon, cholera toxin, and retinoic acid. *J Immunol*. 1981;126:2129–35.

### **Publisher's Note**

Springer Nature remains neutral with regard to jurisdictional claims in published maps and institutional affiliations.